




Gyrotron multistage depressed collector based on $E \times B$ drift concept using azimuthal electric field. II: Upgraded designs

Cite as: Phys. Plasmas **26**, 013108 (2019); <https://doi.org/10.1063/1.5078861>

Submitted: 29 October 2018 . Accepted: 14 December 2018 . Published Online: 22 January 2019

Chuanren Wu (吴传人) , Ioannis Gr. Pagonakis, David Albert, Konstantinos A. Avramidis , Gerd Gantenbein, Stefan Illy, Manfred Thumm , and John Jelonnek 



[View Online](#)



[Export Citation](#)



[CrossMark](#)



Gyrotron multistage depressed collector based on $E \times B$ drift concept using azimuthal electric field. II: Upgraded designs

Cite as: Phys. Plasmas **26**, 013108 (2019); doi: [10.1063/1.5078861](https://doi.org/10.1063/1.5078861)

Submitted: 29 October 2018 · Accepted: 14 December 2018 · Published Online: 22 January 2019



View Online



Export Citation



CrossMark

Chuanren Wu (吴传人), Ioannis Gr. Pagonakis, David Albert, Konstantinos A. Avramidis, Gerd Gantenbein, Stefan Illy, Manfred Thumm, and John Jelonnek

AFFILIATIONS

Institute for Pulsed Power and Microwave Technology, Karlsruhe Institute of Technology, Hermann-von-Helmholtz-Platz 1, 76344 Eggenstein-Leopoldshafen, Germany

ABSTRACT

Multistage Depressed Collectors (MDCs) are nontrivial for high-frequency gyrotrons. A basic conceptual design of an $E \times B$ MDC using azimuthal electric fields was proposed in Part I of this series. In the present work, several upgraded design proposals based on the basic one will be elaborated. These proposals will significantly reduce the back-stream of electrons, which was the main drawback of the basic design proposal. Another upgraded design proposal will shrink the length and maximal radius of the MDC to be only a fraction of its full-length version. A conceptual design of the final MDC proposal will be given at the end.

Published under license by AIP Publishing. <https://doi.org/10.1063/1.5078861>

I. INTRODUCTION

Today's fusion gyrotrons with single-stage depressed collectors have efficiencies of approximately 50%. The DEMOnstration fusion power plant will require gyrotrons to have higher than 60% overall efficiency. A coaxial-cavity gyrotron for DEMO is under an early stage of development,¹ wherein a Multistage Depressed Collector (MDC) will be the key component to achieve the target efficiency. However, the design of a high-power fusion gyrotron MDC is nontrivial. The main reason is the moderate magnetic field in the collector. The magnetic field confines the hollow electron beam in small-orbits and prevents the electron trajectories from spreading. Two fundamentally different concepts for (small-orbit) gyrotron MDCs exist: the axisymmetric concept²⁻⁴ and the concept based on the $E \times B$ drift.⁵⁻¹¹ Numerical studies have shown that the latter might have more advantages than the former, especially when their sizes, efficiencies, and the influences of secondary electrons are compared. There are several approaches to produce the $E \times B$ drift in a collector, as explained in Part I of this work.¹¹ Among the various approaches, the design of a two-stage depressed collector using azimuthal electric fields to create a radial drift^{5,9-11} is worthy of being further investigated and realized.

In order to have a relatively invariable reference, the MDC examples in this publication series are considered for

the magnetic field and the spent electron beam of an existing high-power fusion gyrotron such as the experimentally well-tested 170 GHz 1 MW TE_{32,9}-mode (hollow-cavity) gyrotron.¹² Whether there is a coaxial insert in the cavity should not affect the physical principle of the proposed MDC concept, except that the collector geometry, the magnetic field, and the potential of the stages may need to be tuned for a different gyrotron. The 170 GHz 1 MW reference gyrotron operates with an acceleration voltage of approximately 70 kV and a beam current of 45 A. Its interaction efficiency is expected to be 35%, which means that the targeted collector should be able to recuperate at least 74% of the spent beam power, in order to achieve a gyrotron overall efficiency of higher than 60%. The energy distribution of the spent electron beam visualized in Fig. 1 is obtained from the interaction simulations by EURIDICE.¹³

The MDC proposal in Part I of this publication series belongs to the approach using the azimuthal electric field. Simulations of that design show a collector efficiency of 77%. This part of the publication series proposes two kinds of upgraded designs based on the original one of Part I. In particular, the electron back-stream of the original design can be suppressed and the size of the collector can be notably reduced. As a side effect, the collector efficiency increases further to 78% due to the proper collection of the originally back-streamed

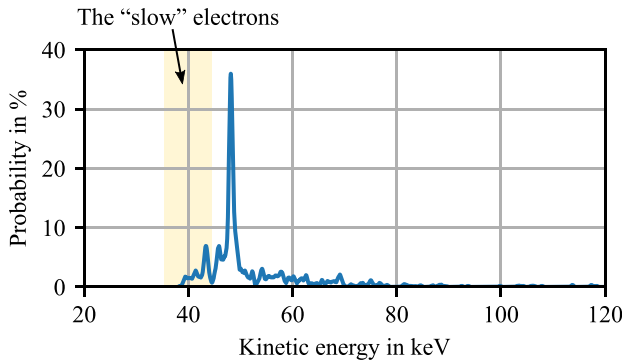


FIG. 1. Simulated energy distribution of the spent electron beam.

beam current, although the efficiency improvement is not the main purpose of these upgraded design proposals.

There was a back-streamed beam current of 700 mA in the original MDC design. It is caused by the fact that the azimuthal electric field has to change its sign at a certain azimuthal angle, in order to fulfill

$$\nabla \times \mathbf{E} = -\frac{\partial \mathbf{B}}{\partial t} = 0. \tag{1}$$

As the azimuthal electric field flips, the radial $\mathbf{E} \times \mathbf{B}$ drift also reverts its direction. In Fig. 2, this special azimuthal position of the MDC is shown. There is a straight gap joining both ends of the helical gap. In the azimuthal range close to that straight gap, the $\mathbf{E} \times \mathbf{B}$ drift does not guide the initially slow electrons (marked in Fig. 1) to the first stage. Consequently, these slow electrons cannot overcome the depression voltage at the second stage, and thus, they form a back-stream current. Although it has been observed in the experiments^{14,15} of single-stage depressed collectors and also in full-gyrotron simulations that a small amount of back-stream current does not affect the gyrotron operation too much, in order to reduce the risk, the back-stream current should be suppressed.

On the one hand, this back-stream current can be reduced by minimizing the width of that straight gap in Fig. 2. However, this kind of optimization does not fundamentally solve the issue. On the other hand, the operation principle of the original design in Part I could be improved, such that back-stream electrons can be prevented from the principle. This paper will consider the second case.

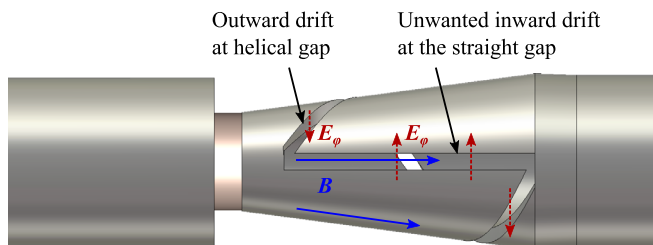


FIG. 2. The unwanted inward drift at the azimuthal angle of the straight gap in the original design proposal presented in Part I.

Section II presents four upgraded designs which will minimize the back-stream current. After the issue of back-stream is solved with these proposals, another upgraded design, which can minimize the collector length, is presented in Sec. III. Simulations are performed using CST Particle Studio, where both secondary electrons (using the Furman model¹⁶ for copper implemented in CST) and space charge effects are taken into account. Finally, a conceptual design is given in Sec. IV.

II. UPGRADED DESIGN PROPOSALS FOR THE MINIMIZATION OF THE ELECTRON BACK-STREAM

The goal of the design proposals in this section is to prevent low-energetic electrons from being back-streamed (reflected) at the azimuthal angle of the straight gap, without sacrificing the collector efficiency. In addition, one advantage of the original design is that it makes use of the gyrotron decaying magnetic field and requires relatively simple tuning coils. This feature should be preserved in the upgraded designs.

Therefore, the most appropriate way to suppress the back-stream current is to change the electric field or to modify the geometry of the original design. There are four particular proposals for the geometry modification.

A. Proposal 1: Introducing an azimuthal drift

The first approach is to avoid electrons staying in the range of the straight gap. Electrons, especially the slow ones at the straight gap, will be cleared with an additional drift, before they would be reflected. These electrons have to drift azimuthally to the side of the first stage. To create this drift, an additional radial electric field has to be applied. This electric field is located between the original collector wall (where the helical gap is located) and the newly inserted electrode on the axis.

Figure 3 shows the principle of this upgraded design proposal. Another conic electrode is coaxially inserted into the original collector structure. It has the same potential as the second

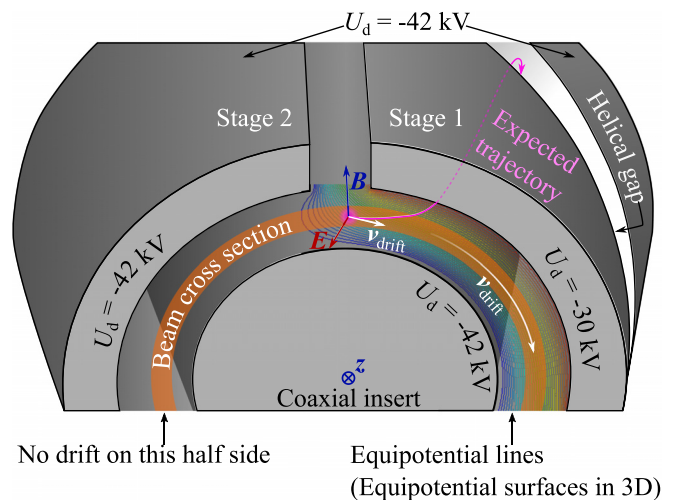


FIG. 3. Schematic cut view of the first proposal for the minimization of the electron back-stream.

(last) collector stage and thus can be hung on the top of the second stage without additional isolation of electric potentials. U_d is the deceleration voltage relative to the gyrotron body (cavity). As the inserted structure is not on the path of electron trajectories, there should be theoretically no beam current collected at this component. Hence, only the outer surface of this conic structure is necessary. In the simulation, a simplified bulky geometry like in Fig. 3 can facilitate the mesh generation.

The cross section of the spent electron beam with a finite beam width is presented qualitatively as the orange ring in Fig. 3, while the electron beam is marching along the $+z$ axis. A drift affects the electrons at the position marked in magenta. This drift follows the equipotential lines (equipotential surfaces in 3D) toward the right half side of this view. With this drift, (slow) electrons will leave the region under the straight gap and approach the helical gap at another azimuthal angle, as shown by the magenta trajectory. There, they will be normally sorted by the $\mathbf{E} \times \mathbf{B}$ drift. Those electrons, which are originally at the right half side of this cross section, are also affected by the azimuthal drift. They will drift clock-wise and will be collected at the helical gap on another azimuthal angle. On the other hand, the left half part of the electron beam in this figure has already passed the helical gap and therefore the electrons are only those initially having a high energy. They will be collected at the second stage. There will be no azimuthal or radial electric field (except a negligible electric field from the space charge of the electron beam) affecting those electrons (no equipotential line is drawn in this region). Therefore, those electrons are not affected by this geometrical upgrade.

The simulation of this upgraded design predicts 1.1% back-stream current (500 mA of 45 A), no matter whether secondary electrons are taken into account. This is better than the situation in the original design, which had a back-stream of 700 mA, but the back-stream currents in both cases are still in the same order of magnitude. There can be multiple reasons that this configuration does not suppress the back-stream effectively. First, the azimuthal drift may not be strong enough for this particular simulation. Second, the electrons near to the left edge of the straight gap may still undergo a bad condition: they will drift to a small radius near to the inserted electrode, where the depression voltage U_d is high (i.e., potential is very negative). Then, the low-energetic fraction of these electrons will be reflected.

B. Proposal 2: Increasing the helix angular range

The angular range of the helix in the original design was slightly less than 2π . If the angular range of the helix is broader than 2π , one can make use of this additional angle to "hide" (a large part of) the inward drift region behind a helical gap for the normal $\mathbf{E} \times \mathbf{B}$ collection. The idea is shown in Fig. 4.

Here, both ends of the helix are not at the same azimuthal angle. The original straight gap is split into two segments. The segment at the beginning of the collector is shorter, while the other is significantly longer. The $\mathbf{E} \times \mathbf{B}$ drifts at the straight gaps remain inward. However, the inward drift at the short segment affects the electrons only for a short time duration, such that the electrons will hardly leave their magnetic flux surface until they are sorted near the end of the collector by the last piece of

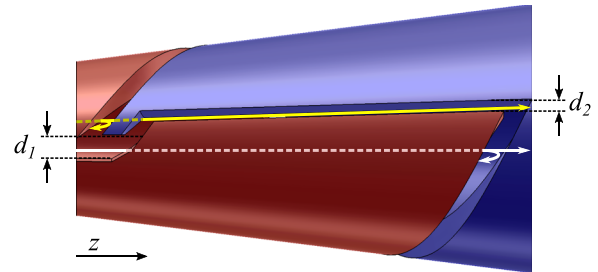


FIG. 4. Schematic of the second proposal for the minimization of the electron back-stream.

helical gap (see the white trajectory in Fig. 4). For simplicity, the long segment of the inward-drift gap remains straight and aligned; however, it is in another azimuthal angle. At the latter azimuthal angle, although the inward drift affects the electron beam for a long distance, it will not reflect beam electrons, since the slow electrons have already been split out of the beam at the beginning of the collector, as shown by the yellow trajectory in Fig. 4. Moreover, the width of the first gap d_1 can be large, in order to further decrease the effect of the inward drift at the short segment.

Depending on the setup, this improved design still has a 150 ± 80 mA back-stream current of the total 45 A injected current, shown by simulations. The back-stream current is significantly reduced, compared to the original 700 mA. So, it seems that this proposal is better for suppressing back-stream electrons than the first one.

One important reason for the tenacious back-stream electrons can be explained with the beam cross section given in Fig. 5. Let α be the azimuthal range of the straight gap and β the angular range where electrons are drifting inwards. α is almost constant along the collector, while β increases as z is increasing.

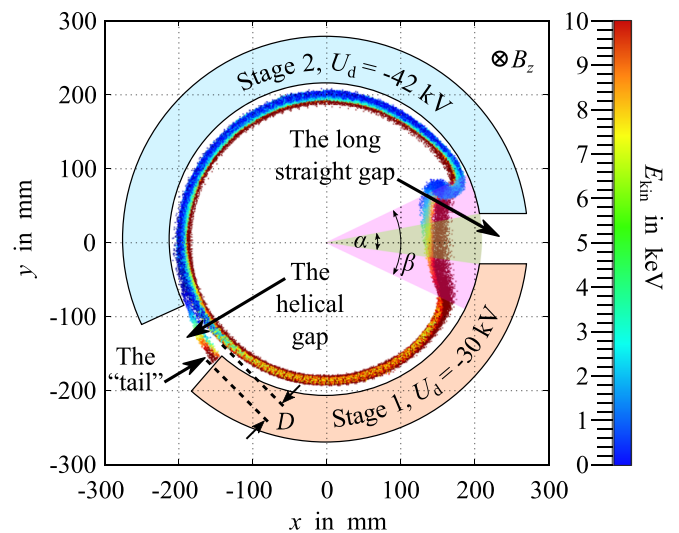


FIG. 5. Cross section of the electron beam;¹¹ the "tail" of the beam rotates clockwise around the center of cross section and the angle β grows as z increases.

If the azimuthal position of the short segment is covered by the angle β before the end of the helix, then the electrons at that azimuthal positions need more outward drift to be sorted at the helix; otherwise, the slow electrons will be reflected. Unfortunately, this situation cannot be managed just by adjusting the parameters. For example, adding more azimuthal angle to the helix separates the long and short straight segments further away from each other. However, to keep the same torsion (therefore, same drift), the collector has to be longer, while a longer collector means a larger angle β at the end of the helix. The new β at the end of the collector covers again the azimuthal position of the short segment, which has been rotated away though. Then, one comes back to the same situation. To solve this issue, the principle has to be enhanced as will be shown in Secs. II D and III.

C. Proposal 3: Collecting the reflections by a disk

As the reflected electrons are close to the axis, they can be captured by an additional electrode on their return path. This electrode has the form of a disk for simplicity and is held from the end of the collector, as shown in Fig. 6. The trajectory of an originally reflected slow electron at the azimuthal angle of the straight gap is illustrated in the figure. The radial distance from the annular beam to the disk is similar to the one between electron beam and the collector inner wall, such that the electron beam can enter the MDC as in the original design.

Simulations show that this additional disk reduces the back-stream current from 700 mA to approximately 200 mA, which is as effective as the upgrade in Sec. II B. The remaining reflected electrons are mainly those ones with an insufficient drift (both inward and outward) around the angle of the straight gap. The disk will have to absorb 2.4 kW beam power (will be reduced with the upgrade in Sec. II D) in the reference example. Cooling of the disk has to be considered via the hanging support structure.

D. Proposal 4: The combination of proposals 2 and 3

This proposal combines the previous ones from Secs. II B and II C. Thus, it

- suppresses the back-stream current more than any of the two proposals individually,
- relaxes the cooling requirement of the coaxial disk.

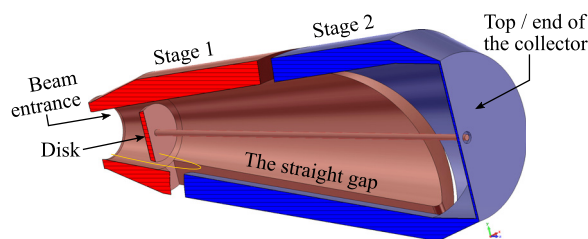


FIG. 6. Schematic of the third proposal for the minimization of the electron back-stream.

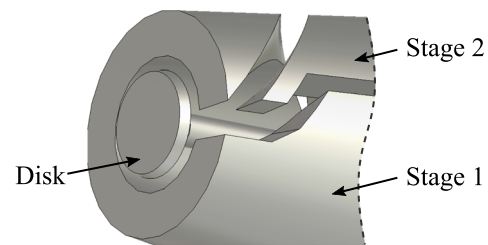


FIG. 7. Front part of the combined proposal for the minimization of the electron back-stream.

Figure 7 shows the structure of the front part (collector entrance). Simulations of this structure verified the speculations, such that the reflected current is reduced to 20–30 mA (including secondary electrons), which could be acceptable in the gyrotron operation. In the worst case, 100 mA (up to 1 kW) is collected at the disk, which is halved compared to the uncombined version. Since the current collected by the disk only consists of a tiny part of the total electron beam, evaluating an accurate thermal loading of these electrons requires a very fine sampling of the reflected electron beam. Hence, the total input electron beam should be sampled with an extremely high number of electrons. That would demand too much computational resource and will be further investigated.

The flaw of the original MDC design in Part I of this publication series has been so far remedied, for the price of a structure modification.

E. Further investigation: Segmented electron beam

Besides these four approaches, the so-called segmented beam¹⁷ could also be a candidate for the suppression of the back-stream current. For this study, possible instabilities of such a non-axisymmetric electron beam are not considered. The idea is to disable (e.g., coat) one sector of the emitter ring or use a segmented gyrotron emitter,¹⁸ so that there is no electron at a certain azimuthal angle. Aligning this angle to the straight gap (taking into account also the azimuthal drift inside a gyrotron), there should be no electron at that angle in the collector, and thus, no electron would be reflected. However, the angle β shown in Fig. 5 is not of the same order as the supposed angular range of the non-emitting sector. Therefore, the segmented beam may not be the best solution.

III. UPGRADED DESIGN PROPOSAL FOR THE REDUCTION OF THE COLLECTOR SIZE

Based on the previous proposals, another upgraded MDC design will be proposed in this section. It will lead to a notable reduction of collector size (both the length and the maximal radius), such that the size of the new design will be only a fraction of the original one.

Figure 8 shows the schematic of this upgraded MDC design. It applies the scheme of Sec. II D to prevent beam electrons from back-streaming, while instead of a single helical gap around the azimuthal angle, there are multiple ones. In this example, each helical structure has only 1/3 of the original (axial)

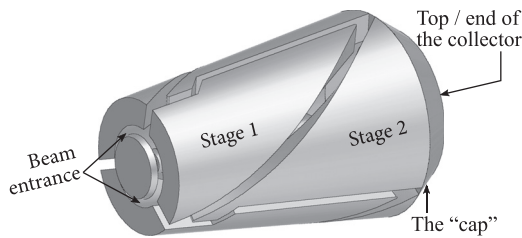


FIG. 8. The collector size can be reduced by repeating the helical gap azimuthally.

length but repeats itself three times azimuthally. The total collector length including the "cap" of the second stage is approximately 50 cm. The torsion of the helices (i.e., the angle between the electric and magnetic fields), electric potentials (depression voltages), and the magnetic flux density are preserved as in Sec. II D. Therefore, the properties of the $\mathbf{E} \times \mathbf{B}$ drift, in particular, the drift distance D (marked in Fig. 5), are the same as the design in Sec. II D, although the total collector length is reduced. As the maximal radius of the conic structure depends on the cone length, reduction of the collector length also results in a reduction of the maximal radius at the end of the conic collector. The peak power density at the first stage is not changed. At the second stage, the power density will be higher than in the full-length version, since the maximal radius is reduced. The current reference value of 500 W/cm^2 will be exceeded. Therefore, a local beam sweeping only at the second stage should be considered. The sweeping coil will be placed at the end (top) of the collector. The magnetic field at the end of collector where the sweeping is required is weaker than that in the conic region. A weak sweeping magnetic field (in the range of mT) is significant to the field in the end region but not to the field at the entrance or in the conic region for the $\mathbf{E} \times \mathbf{B}$ drift (there, the field is tens of mT). In addition, the sweeping coil is far from the conic part, such that the perturbation to the field in the conic region is further reduced. Therefore, a carefully designed sweeping magnetic field will not affect the functionality of the $\mathbf{E} \times \mathbf{B}$ drift in the conic region.

Besides the size reduction, this upgrade has two other advantages. First, the angle β (see Fig. 5) will be closer to α , because the effects (especially the drift distance) produced by the inward drift depend on the time for which the electrons are exposed to this drift. This time duration is related to the collector length. A small β will facilitate the optimization. Second, the collector coil system can be simplified. Originally in the design shown in Part I, three normal-conducting coils are required to tune the magnetic field in the collector region; as the collector becomes shorter, less tuning coils are required. In addition, it is more feasible to collimate the local curvature of magnetic field lines to match the conic structure than over a longer axial range.

Simulations predict the same collector efficiency as the full-length candidates. A back-stream current of 41.4 mA including secondary electrons from the 45A input spent electron beam is observed in the simulation (while 22.5 mA if secondary electrons are ignored in the simulation). A current of 37 mA is collected at the disk, which results in a total power of 400 W

distributed in the shape of sickles at three sectors on the disk. The average load (total power/area of the disk) is very low. However, the collection of high-energetic electrons at the second stage causes a high thermal load, see the discussion in Part I. For long-pulse gyrotron operation, the electron beam should be locally swept at the "cap" cylinder of the second stage.

IV. CONCEPTUAL DESIGN

A conceptual MDC was designed based on the idea presented in Sec. III for the experimental validation in the next step. The insulation scheme of a typical fusion gyrotron is considered in this design, which means that the cavity is at a positive body potential (approximately 30 kV) while the mirror-box and the collector outer case [i.e., the vacuum envelope (b) in Fig. 9] are grounded to create a depression voltage for the first stage. The possibility of applying a water-cooling system can be considered also in short-pulse operations, in order to increase the duty circle. The surfaces of the first stage are thin metal plates supported by a metal frame. There are cooling pipes (d) beneath the helical surface (c) at the first stage in order to dissipate the beam energy of the slow electrons (up to 42 keV initial kinetic energy). The cooling water is fed through the pipes (a). (e) is the coaxial rod, which is also grounded and hung from the top of the vacuum envelope.

The second stage has a potential of -12 kV . It is lifted by the insulators (f). (g) is the "cap" of the second stage, which can also be water cooled. The water is fed via the ceramic pipe (h), which insulates also the ground potential and the potential of the second stage. To protect the second stage from harmful transverse motions, which may break the insulators, ceramic blocks (i) are used to fix the transverse position of the second stage. In total, the collector will weight approximately 300 kg.

V. CONCLUSIONS

Multistage depressed collectors for gyrotrons are challenging. The design proposed in Part I of this publication series is a very promising approach. However, there was theoretically a small amount of electron beam current back-streamed to gyrotron cavity. To suppress this current, four upgraded designs are

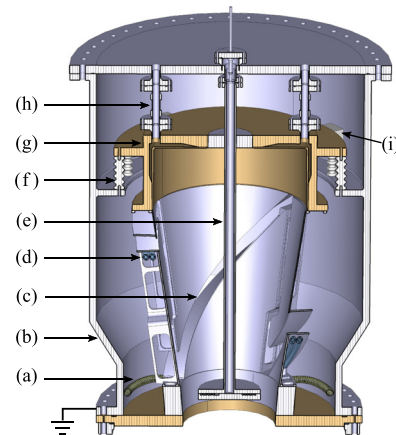


FIG. 9. Cut-view of the conceptual design for the upgraded MDC.

presented. Simulations for the 170 GHz 1 MW gyrotron with a total input electron beam current of 45 A show that the best design can reduce the back-stream current from 700 mA to approximately 20 mA only.

As the electron back-stream is suppressed, the size of the MDC can be significantly reduced if the helical gap for the energy-sorting is repeated azimuthally. Reducing the MDC length also simplifies the tuning coils for the collector. A conceptual design of the MDC is presented.

ACKNOWLEDGMENTS

This work was carried out within the framework of the EUROfusion Consortium and received funding from the Euratom research and training programme 2014–2018 and 2019–2020 under Grant Agreement No. 633053. The views and opinions expressed herein do not necessarily reflect those of the European Commission.

REFERENCES

- ¹J. Jelonnek, G. Aiello, S. Alberti, K. Avramidis, F. Braunmueller, A. Bruschi, J. Chelis, J. Franck, T. Franke, G. Gantenbein, S. Garavaglia, G. Granucci, G. Grossetti, S. Illy, Z. C. Ioannidis, J. Jin, P. Kalaria, G. P. Latsas, I. G. Pagonakis, T. Rzesnicki, S. Ruess, T. Scherer, M. Schmid, D. Strauss, C. Wu, I. Tigelis, M. Thumm, and M. Q. Tran, "Design considerations for future DEMO gyrotrons: A review on related gyrotron activities within EUROfusion," *Fusion Eng. Des.* **123**, 241–246 (2017).
- ²M. E. Read, W. G. Lawson, A. J. Dudas, and A. Singh, "Depressed collectors for high-power gyrotrons," *IEEE Trans. Electron Devices* **37**, 1579–1589 (1990).
- ³A. Singh, G. Hazel, V. L. Granatstein, and G. Saraph, "Magnetic field profiles in depressed collector region for small-orbit gyrotrons with axial or radially extracted spent beam," *Int. J. Electron.* **72**, 1153–1163 (1992).
- ⁴A. Singh, S. Rajapatirana, Y. Men, V. L. Granatstein, R. L. Ives, and A. J. Antolak, "Design of a multistage depressed collector system for 1-MW CW gyrotrons. I. trajectory control of primary and secondary electrons in a two-stage depressed collector," *IEEE Trans. Plasma Sci.* **27**, 490–502 (1999).
- ⁵I. G. Pagonakis, J. P. Hogge, S. Alberti, K. A. Avramides, and J. L. Vomvoridis, "A new concept for the collection of an electron beam configured by an externally applied axial magnetic field," *IEEE Trans. Plasma Sci.* **36**, 469–480 (2008).
- ⁶O. I. Louksha and P. A. Trofimov, "A method of electron separation for multistep recuperation systems in gyrotrons," *Tech. Phys. Lett.* **41**, 884–886 (2015).
- ⁷I. G. Pagonakis, C. Wu, S. Illy, and J. Jelonnek, "Multistage depressed collector conceptual design for thin magnetically confined electron beams," *Phys. Plasmas* **23**, 043114 (2016).
- ⁸C. Wu, I. G. Pagonakis, G. Gantenbein, S. Illy, M. Thumm, and J. Jelonnek, "Conceptual designs of E×B multistage depressed collectors for gyrotrons," *Phys. Plasmas* **24**, 043102 (2017).
- ⁹C. Wu, I. G. Pagonakis, S. Illy, G. Gantenbein, M. Thumm, and J. Jelonnek, "Novel multistage depressed collector for high power fusion gyrotrons based on an E×B drift concept," in *Proceedings of the International Vacuum Electronics Conference (IVEC)* (2017), pp. 1–2.
- ¹⁰C. Wu, I. G. Pagonakis, G. Gantenbein, S. Illy, M. Thumm, and J. Jelonnek, "Design of E×B multistage depressed collector concepts for high-power fusion gyrotrons," in *42nd International Conference on Infrared, Millimeter, and Terahertz Waves (IRMMW-THz)* (IEEE, 2017), pp. 1–2.
- ¹¹C. Wu, I. G. Pagonakis, K. A. Avramidis, G. Gantenbein, S. Illy, M. Thumm, and J. Jelonnek, "Gyrotron multistage depressed collector based on E×B drift concept using azimuthal electric field. I. basic design," *Phys. Plasmas* **25**, 033108 (2018).
- ¹²T. Rzesnicki, F. Albajar, S. Alberti, K. A. Avramidis, W. Bin, T. Bonicelli, F. Braunmueller, A. Bruschi, J. Chelis, P.-E. Frigot, G. Gantenbein, V. Hermann, J.-P. Hogge, S. Illy, Z. C. Ioannidis, J. Jin, J. Jelonnek, W. Kasperek, G. P. Latsas, C. Lechte, M. Lontano, T. Kobarg, I. G. Pagonakis, Y. Rozier, C. Schlatter, M. Schmid, I. G. Tigelis, M. Thumm, M. Q. Tran, J. L. Vomvoridis, and A. Zisis, "Experimental verification of the European 1 MW, 170 GHz industrial CW prototype gyrotron for ITER," *Fusion Eng. Des.* **123**, 490–494 (2017).
- ¹³K. A. Avramides, I. G. Pagonakis, C. T. Iatrou, and J. L. Vomvoridis, "EURIDICE: A code-package for gyrotron interaction simulations and cavity design," in *European Physical Journal Web of Conferences* (2012), Vol. 32, p. 04016.
- ¹⁴K. Sakamoto, M. Tsuneoka, A. Kasugai, T. Imai, T. Kariya, K. Hayashi, and Y. Mitsunaka, "Major improvement of gyrotron efficiency with beam energy recovery," *Phys. Rev. Lett.* **73**, 3532–3535 (1994).
- ¹⁵B. Piosczyk, C. T. Iatrou, G. Dammertz, and M. Thumm, "Single-stage depressed collectors for gyrotrons," *IEEE Trans. Plasma Sci.* **24**, 579–585 (1996).
- ¹⁶M. A. Furman and M. T. Pivi, "Probabilistic model for the simulation of secondary electron emission," *Phys. Rev. Spec. Top. Accel. Beams* **5**, 124404 (2002).
- ¹⁷M. E. Read, A. J. Dudas, J. J. Petillo, and M. Q. Tran, "Design and testing of an electron gun producing a segmented sheet beam for a quasi-optical gyrotron," *IEEE Trans. Electron Devices* **39**, 720–726 (1992).
- ¹⁸A. Malygin, S. Illy, I. G. Pagonakis, B. Piosczyk, S. Kern, J. Weggen, M. Thumm, J. Jelonnek, K. A. Avramides, R. L. Ives, D. Marsden, and G. Collins, "Design and 3-D simulations of a 10-kW/28-GHz gyrotron with a segmented emitter based on controlled porosity-reservoir cathodes," *IEEE Trans. Plasma Sci.* **41**, 2717–2723 (2013).